

Laboratory For Atmospheric and Space Physics

LASP Engineering Division
University of Colorado
Boulder, Colorado



Solar Dynamics Observatory
EUV Variability Experiment
(SDO EVE)

Calibration and Measurement Algorithms Document (CMAD)

Document No. **EVE-T-11003** Rev. **A** Date: 01/31/2005

Prepared By: Francis G. Eparvier, EVE Project Scientist

Revision History				
Rev	Description of Change	By	Approved	Date
1	Draft for PDR	FGE	TNW	12/13/2003
A	Revised Draft for CDR	FGE	TNW	1/31/2005

CHECK TO VERIFY THAT THIS IS THE CURRENT VERSION PRIOR TO USE

Authority	Signature	Date
Approved by	 Francis G. Epurvie, EVE Project Scientist	01-Feb-2005
Approved by	 Thomas N. Woods, EVE Principal Investigator	01-Feb-2005
Approved by	 Andrew R. Jones, EVE Instrument Scientist	2/2/2005
Approved by	 Mike Antinson, EVE Project Manager	2/1/05
Approved by	 Greg Ucker, EVE Systems Engineer	2/2/05

CM FOREWORD

This document is a Solar Dynamics Observatory EUV Variability Experiment project controlled document. Changes to this document require prior approval of the EVE project. Proposed changes shall be submitted to EVE Configuration Management, along with supportive material justifying the proposed change.

Questions or comments concerning this document should be addressed to:

EVE Configuration Manager
Laboratory for Atmospheric and Space Physics
University of Colorado
1234 Innovation Dr.
Boulder, CO 80303

Table of Contents

1	Scope.....	1
2	Related Documentation.....	1
2.1	Applicable Documents.....	1
3	Overview and Background Information.....	1
3.1	Science Objectives.....	1
3.2	EVE Instrument Description.....	2
3.2.1	Overall EVE Measurement Concept.....	2
3.2.2	EVE Instrument Subsystem Descriptions.....	4
3.2.2.1	Multiple EUV Grating Spectrographs (MEGS).....	4
3.2.2.1.1	MEGS Channel A (MEGS-A) Design.....	4
3.2.2.1.2	MEGS Channel B (MEGS-B) Design.....	6
3.2.2.1.3	MEGS Solar Aspect Monitor (MEGS-SAM) Design.....	8
3.2.2.1.4	MEGS Photometer (MEGS-P) Design.....	9
3.2.2.1.5	EUV SpectroPhotometers (ESP) Design.....	9
3.2.3	EVE Heritage.....	10
3.2.3.1	Instrument Heritage.....	10
3.2.3.2	Algorithm and Calibration Heritage.....	10
4	EVE Calibration Plan.....	10
4.1	Overall Calibration Scheme.....	10
4.2	Pre-flight Calibration Plans.....	11
4.2.1	MEGS Pre-flight Calibrations.....	11
4.2.2	ESP Pre-flight Calibrations.....	12
4.3	In-flight Tracking of Short-Term Changes.....	12
4.4	Long-term Absolute Calibration Tracking (Re-Calibration).....	12
4.5	Validation.....	13
5	EVE Measurement Algorithm Descriptions.....	13
5.1	Theoretical Basis.....	13
5.2	Conversion of Instrument Signals to Irradiance Units.....	14
5.2.1	MEGS-A and MEGS-B Measurement Equations.....	14
5.2.2	MEGS-SAM Measurement Equation.....	15
5.2.3	ESP and MEGS-P Measurement Equation.....	15
5.3	Signal Estimates and Error Analyses for Subsystems.....	15
5.3.1	MEGS Signal Estimates and Error Analysis.....	15
5.3.2	MEGS-SAM Signal Estimates and Error Analysis.....	18
5.3.3	ESP Signal Estimates and Error Analysis.....	20
5.4	Preflight Calibration Algorithms.....	20
APPENDIX A: List of EVE Variable Definitions.....		21

List of Tables

Table 1: List of Applicable Documents	1
Table 2: EVE Science Requirements	2
Table 3: MEGS-A and MEGS-B Uncertainty Estimate and Error Budget	18
Table 4: MEGS-SAM Uncertainty Estimate and Error Budget.....	19
Table 5: ESP Uncertainty Estimate and Error Budget.....	20

List of Figures

Figure 1: EVE redundant wavelength coverage diagram.	3
Figure 2: MEGS-A optical layout with MEGS-SAM.....	5
Figure 3: MEGS-A simulated detector image with MEGS-SAM image. Slit 1 is on top and Slit 2 is on the bottom. Note that the image has been contrast-enhanced to show weaker lines. The corresponding solar signal estimate is shown below the image.	6
Figure 4: MEGS-B optical layout.	7
Figure 5: MEGS-B simulated detector image. The primary science (1.1) order spectrum falls diagonally across the detector from the upper right to lower left. Note that the image has been contrast-enhanced to show weaker lines. The corresponding solar signal estimate is shown below the image.....	7
Figure 6: MEGS-SAM optical layout withing the MEGS-A housing.....	8
Figure 7: MEGS-P optical alyouth withing the first chamber of MEGS-B. The photometer is placed on the opposite side of the the 0 th order as the primary spectrum from the MEGS-B first grating.....	9
Figure 8: ESP optical layout.	10
Figure 9: MEGS-A Slit 1 signal estimates for solar minimum, maximum, and flare conditions. 16	16
Figure 10: MEGS-A Slit 2 signal estimates for solar minimum, maximum, and flare conditions.	16
Figure 11: MEGS-B signal estimates for solar minimum, maximum, and flare conditions.	17
Figure 12: MEGS-SAM irradiance signal estimates for solar minimum conditions.....	18

1 Scope

The Calibration and Measurement Algorithm Document (CMAD) describes the overall concept for calibrating the EUV Variability Experiment (EVE) instrument for the Solar Dynamics Observatory (SDO), including preflight and inflight calibrations, and details the algorithms for converting instrument signals to solar spectral irradiances, including signal estimates, error analyses, and error budgets. In addition, the document gives a brief overview of the scientific goals of EVE and an introduction to the instrumentation, but it is not designed to be the only reference for these aspects of EVE and gives only enough detail to understand the calibration plan and measurement algorithms. Other, more detailed, documents describe the EVE instrument design, operations, ground system, and data products. All plans and algorithms are described as they are envisioned or known during the design phase of the EVE project. Future changes in instrument design and understanding of calibrations and algorithms may require modifications to this document.

2 Related Documentation

2.1 Applicable Documents

The following documents and drawings in effect on the day this document was signed shall apply to the extent specified herein. In the event of conflict between this document and any referenced document, this document will govern.

The following is a list of the applicable specifications and publications.

Table 1: List of Applicable Documents

DOCUMENT NUMBER	TITLE	Revision/Date
EVE-T-11001	EVE Science Requirements Document	
EVE-T-11002	EVE Systems Requirements Document	
EVE-S-11314	EVE Science Data Processing Requirements Document	
EVE-T-13010	EVE Performance Verification Plan	
EVE-T-11004	EVE Solar Emission Line Measurement List	

3 Overview and Background Information

3.1 Science Objectives

The Extreme Ultraviolet Variability Experiment (EVE) program for the SDO measures the solar extreme ultraviolet (EUV) irradiance with unprecedented spectral resolution, temporal cadence, accuracy, and precision. In addition, the EVE program incorporates physics-based modeling to advance the understanding of the solar EUV irradiance variations based on magnetic features. The science objectives for EVE are fourfold: (1) Specify the solar EUV spectral irradiance and its variability on multiple time scales (seconds to years); (2) Advance current understanding of how and why the solar EUV spectral irradiance varies; (3) Improve the capability to predict

(nowcast and forecast) the EUV spectral irradiance variability; and (4) Understand the response of the geospace environment to variations in the solar EUV spectral irradiance and the impact on human endeavors.

3.2 EVE Instrument Description

3.2.1 Overall EVE Measurement Concept

In order to fulfill the science objectives of EVE, the measurements of solar EUV irradiance must have high spectral resolution, high accuracy and long-term stability throughout the SDO mission. The science requirements are summarized in Table 2. For the origins of the specific requirements, see the EVE Science Requirements Document, EVE-T-11001. To achieve these requirements, the EVE instrumentation includes multiple channels with different optical designs and detectors and with different techniques for pre-flight calibration and in-flight monitoring of relative sensitivity changes, plus regular sounding rocket flights with nearly identical instruments to track absolute sensitivity changes.

Table 2: EVE Science Requirements

Parameter	Minimum Success Requirements	Comprehensive Success Criteria	Design Goals
λ Range	6 or more emissions to specify the chromosphere, TR, and corona, plus the He II 30.4 nm emission	0.1-105 nm	0.1-105 nm
$\Delta\lambda$ Resolution	0.2 nm for these lines	0.1 nm for 18 or more emissions to specify the chromosphere, TR, and corona, and 5 nm or better elsewhere	0.1 nm
Time Cadence	60 sec	< 20 sec	10 sec
Accuracy	35% for 5 nm intervals and daily average	25% for 5 nm intervals and daily average	20% for brighter emissions
Mission Life	3 years	5 years	5 years, long enough to sample low and high solar activity

The EVE instrument subsystems are described in more detail in the following subsections. The overall concept is illustrated in Figure 1, which shows the wavelength coverage of each of the channels of the EVE instrument suite along with a sample solar spectrum.

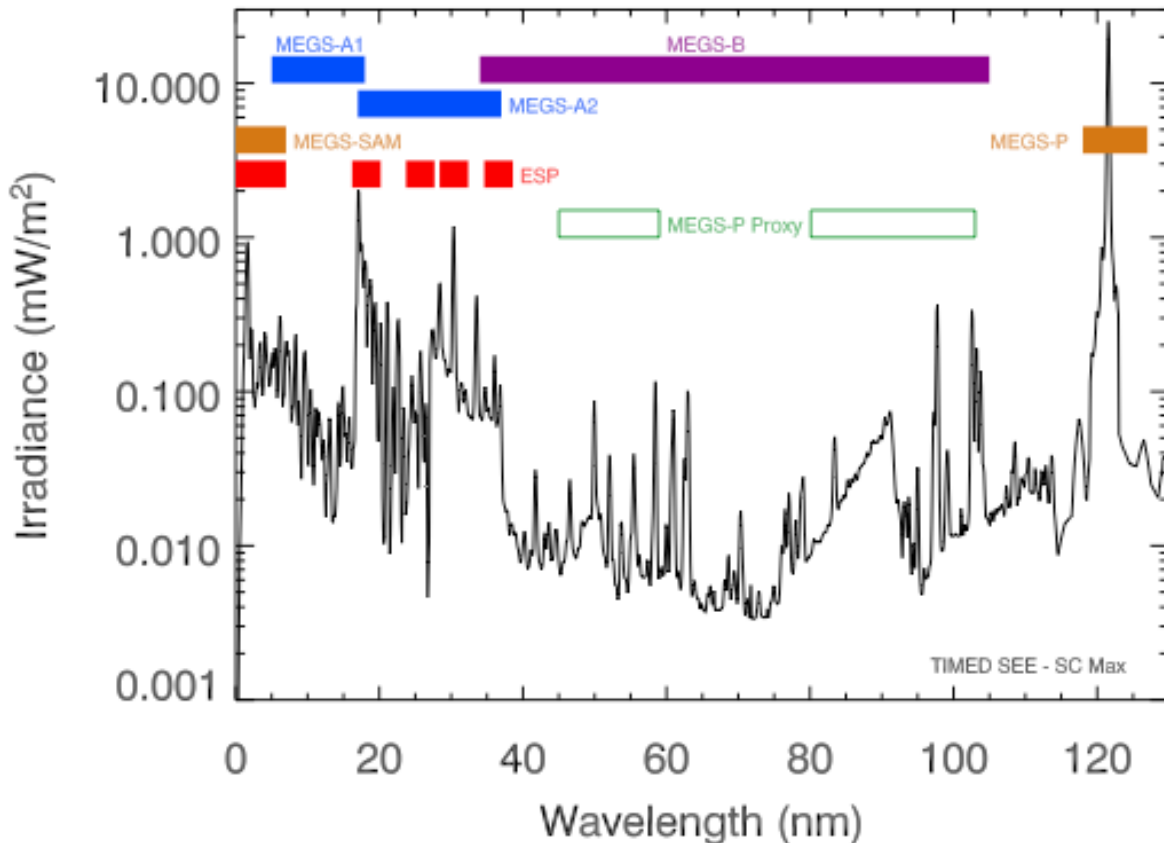


Figure 1: EVE redundant wavelength coverage diagram.

The primary, high spectral resolution irradiance measurements are made by the Multiple EUV Grating Spectrographs (MEGS). The MEGS is composed of two spectrographs: MEGS-A is a grazing incidence spectrograph covering the 5 to 37 nm range, and MEGS-B is a two-grating, cross-dispersing spectrograph covering the 35 to 105 nm range. Included as part of the MEGS-A package, is a pinhole camera to be used as a solar aspect monitor (MEGS-SAM). The MEGS-SAM will provide a pointing reference for the EVE channels. It will also make a spectral measurement of the solar irradiance in the 0.1 to 5 nm wavelength range at approximately 1 nm resolution. In addition, as part of the MEGS-B, is a photodiode with a filter to isolate Lyman- α at 121.6 nm (MEGS-P). This measurement is used for short-term calibration tracking. While Lyman- α is not within the spectral range of the rest of MEGS, it is a proven proxy for other EUV emissions and will be used in conjunction with a spectral model to track potential changes in the sensitivity of the MEGS on the timescale of weeks and months. Longer-term changes in the sensitivity of the EVE channels will be tracked by annual sounding rocket underflights of similar instruments.

Also, for short-term calibration tracking purposes, redundant, lower spectral resolution measurements at select bandpasses will be made by the EUV Spectrophotometer (ESP). The ESP is a transmission grating and photodiode instrument similar to the SOHO SEM. ESP has four channels centered on 18.2, 25.7, 30.4, and 36.6 nm that are each approximately 4 nm in spectral width. The ESP also has a central, zeroth-order diode with a filter to make the primary irradiance measurement in the 0.1 to 7 nm range. The ESP measurements are made at a high time-cadence (0.25 sec) and so are useful as quick indicators of space weather events such as flares.

The redundant wavelength coverage from ESP, the MEGS-P (along with the HI Ly- α proxy) and the MEGS-SAM, all provide EVE with the ability to track any relative sensitivity changes that may occur in the MEGS primary spectral measurements. Absolute sensitivity changes will be provided by sounding rocket underflights of EVE prototype instruments at regular intervals throughout the SDO mission life. The sounding rocket instruments can be calibrated on the ground before and after each rocket flight, and that calibration can be transferred to the EVE instruments on the SDO spacecraft through simultaneous observations.

3.2.2 EVE Instrument Subsystem Descriptions

3.2.2.1 Multiple EUV Grating Spectrographs (MEGS)

The MEGS is an improved version of the EUV Grating Spectrograph (EGS) that is part of the highly successful TIMED SEE instrument [Woods et al., 1998]. The MEGS has two channels: MEGS-A and MEGS-B. Both the EVE MEGS-A and the SEE EGS have spherical grating spectrograph designs that are highly desirable for the EUV range as they require only one reflection. MEGS-A covers the wavelength range from 5 to 37 nm. Unlike the SEE EGS, the EVE MEGS-B uses two normal incidence gratings and covers the wavelength range from 35 to 105 nm. In all these instruments array detectors provide for rapid integration times over the full spectral range. The main improvements over the EGS for MEGS include higher spectral resolution (4 times improvement) that is achieved by having two channels, better sorting of the grating orders, extension to shorter wavelengths, and the use of EUV sensitive CCDs that are more stable with long-term exposures than the MCP-based CODACON detectors used for TIMED EGS.

Both MEGS channels are integrated into the same housing. Each channel is optimized for its respective wavelength range by implementing specific grating angles, coatings on the grating, ruling densities, and filters used in front of the entrance slits. The filters define the desired wavelength ranges and reject out of band contributions, such as visible light. The grating rulings are laminar to suppress higher orders. The MEGS field-of-view (FOV) is 2.0° , which is more than sufficient to measure the off-limb contributions to the irradiance. A study of SOHO EIT images indicates that a FOV of 0.9° is required to measure $> 98\%$ of the solar EUV irradiance. The CCD cameras for MEGS use the MIT LL CCID-28, which is a backside illuminated 2048x1024 CCD.

Each MEGS channel has LED lamps to allow for flatfield characterization of the CCD detectors before and during flight. Each MEGS channel also has a filter wheel to place special filters, instead of the primary science filters, in front of the aperture allowing for characterization of higher order signals before and during flight. The filter wheels also contain dark, or closed aperture, positions to allow for determination of detector dark signals.

In addition to the two spectral channels for MEGS, a Solar Aspect Monitor (MEGS-SAM) has been incorporated into the MEGS-A channel to provide pointing information both during calibration and in-flight. The MEGS-SAM will also provide spectral information between 0.1 and 7 nm.

3.2.2.1.1 MEGS Channel A (MEGS-A) Design

The optical layout of the MEGS-A is shown in Figure 2. It is a 80° grazing incidence, off-Rowland circle spectrograph with a CCD detector to measure the solar spectrum between 5-37

nm at a resolution just less than 0.1 nm. MEGS-A has two entrance slits, each 20 microns wide and 2 mm high, oriented top-to-bottom. In front of the slits is a filter wheel mechanism with bandpass-limiting thin foil (filters made by Luxel). The primary science filters are Zr/C for slit 1 to isolate 5 to 18 nm and Al/Ge/C for slit 2 to isolate 17-37 nm. Secondary filters are available to further limit the bandpasses of each slit to provide an occasional check on higher orders (Zr/Si/C for slit 1 to pass 13 to 18 nm, and Al/Mg/C to pass 25 to 37 nm for slit 2). The filter wheel mechanism also has a blanked-off position for dark measurements. The grating, produced by J.-Y., is a spherical holographic grating with a radius of curvature of 600 mm, platinum coating, and 767 grooves/mm with a laminar groove profile to suppress even orders. The detector for MEGS-A is a back-thinned, back-illuminated, split-frame transfer CCD with 1024x2048 pixels and is being designed and built by MIT-LL. The CCD is maintained at -90°C to suppress noise and to minimize radiation damage in the geosynchronous environment.

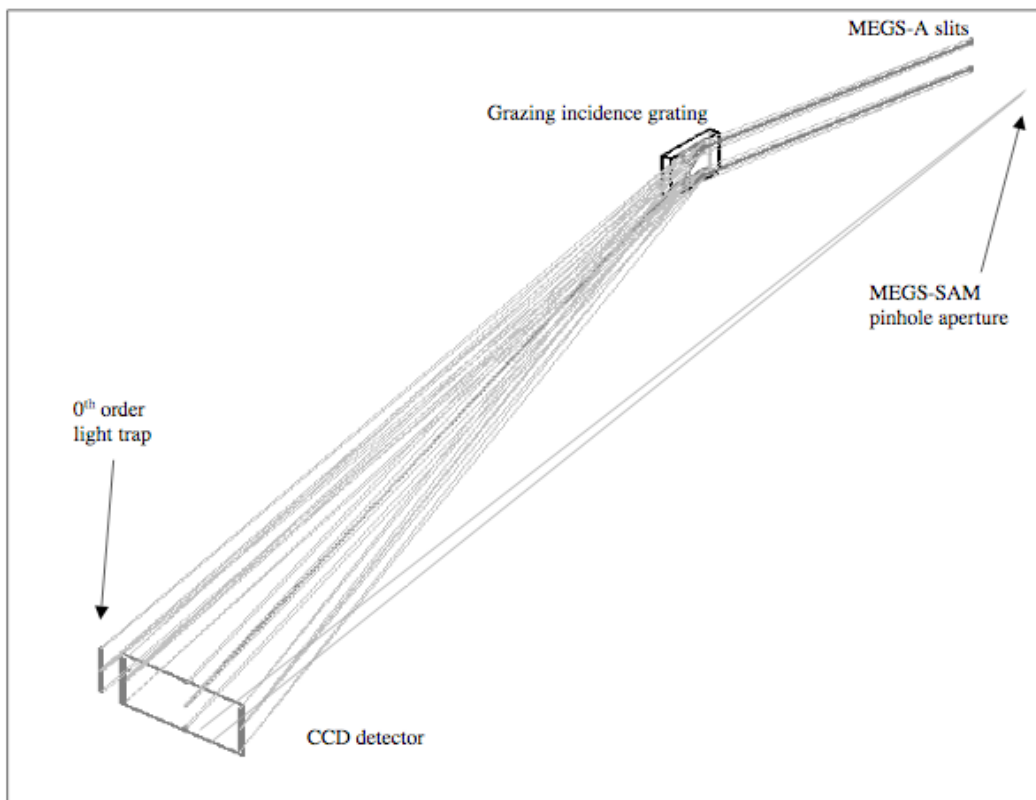


Figure 2: MEGS-A optical layout with MEGS-SAM.

A simulated CCD image of a solar spectrum taken with MEGS-A is shown in Figure 3. The contrast has been enhanced to show dim lines. Wavelengths go from right to left, as indicated on below the image. MEGS-A Slit 1 (upper portion) will be used to cover 5 to 20 nm, and Slit 2 (lower portion) will be used to cover 17 to 37 nm.

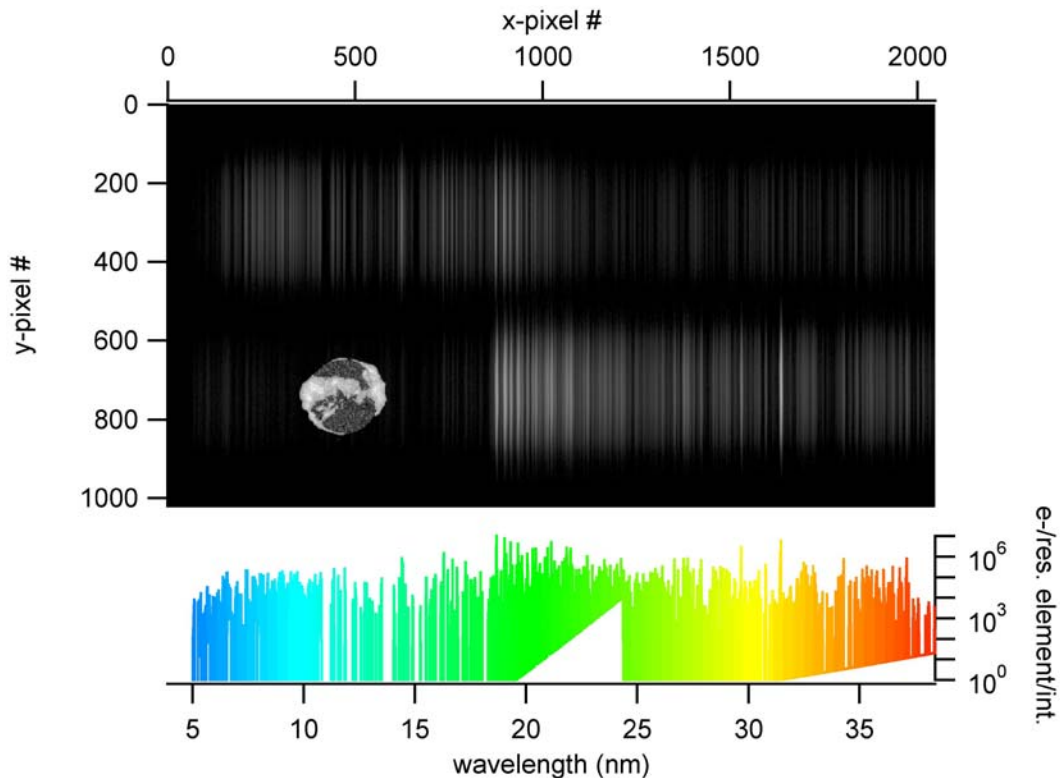


Figure 3: MEGS-A simulated detector image with MEGS-SAM image. Slit 1 is on top and Slit 2 is on the bottom. Note that the image has been contrast-enhanced to show weaker lines. The corresponding solar signal estimate is shown below the image.

3.2.2.1.2 MEGS Channel B (MEGS-B) Design

The optical layout for MEGS-B is shown in Figure 4. MEGS-B is a normal incidence, double-pass, cross-dispersing Rowland Circle spectrograph with a CCD detector to measure the solar spectrum between 35-105 nm at a resolution just less than 0.1 nm. MEGS-B has a single entrance slit, 35 microns wide and 3.5 mm high. The double-pass grating design is needed for MEGS-B to block out unfiltered visible solar light entering the instrument (stable foil filters that pass wavelengths longward of 80 nm do not exist). Reflection gratings typically have 10⁻⁵ to 10⁻⁸ rejection of out-of-band light, with holographically-ruled gratings performing better than mechanically-ruled gratings. The two gratings in MEGS-B reject 10⁻¹⁰ or better of the visible light. The MEGS-B gratings are cross-dispersed giving a spectrum diagonally across the detector with higher order spectra parallel to the main (1st order) spectrum. Both MEGS-B gratings are also produced by J.-Y., and are spherical holographic gratings with platinum coating, and laminar groove profiles to suppress even orders. The first grating has 900 grooves/mm and the second has 2140 grooves/mm. The detector for MEGS-B is identical to the MEGS-A detector. While MEGS-B does not have a primary bandpass filter, it does have a filter wheel in front of the slit. The filter wheel provides an open position for solar measurements, a closed position for detector dark measurements, and a higher order contributions filter (Sn/Ge/SnO₂) for pre-flight calibrations and in-flight checks.

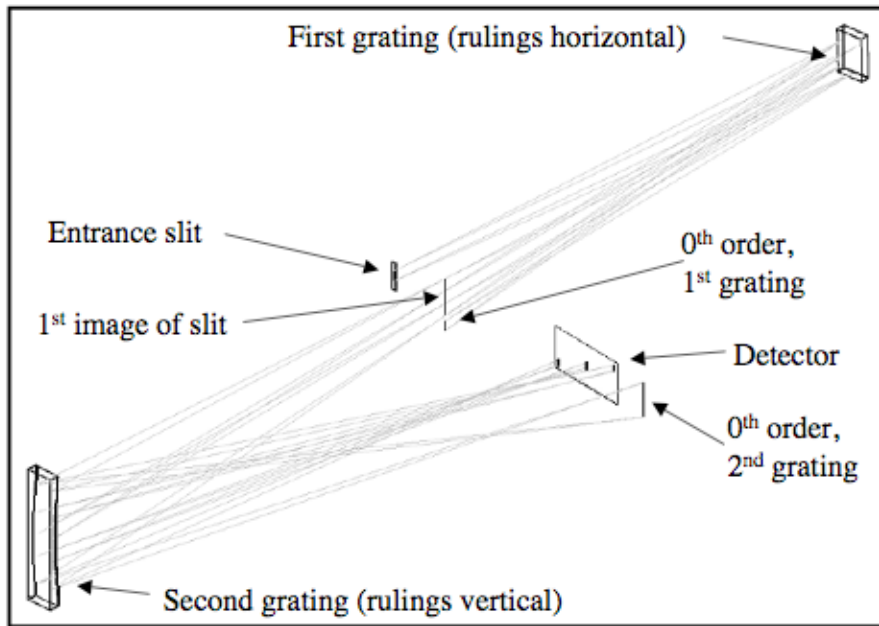


Figure 4: MEGS-B optical layout.

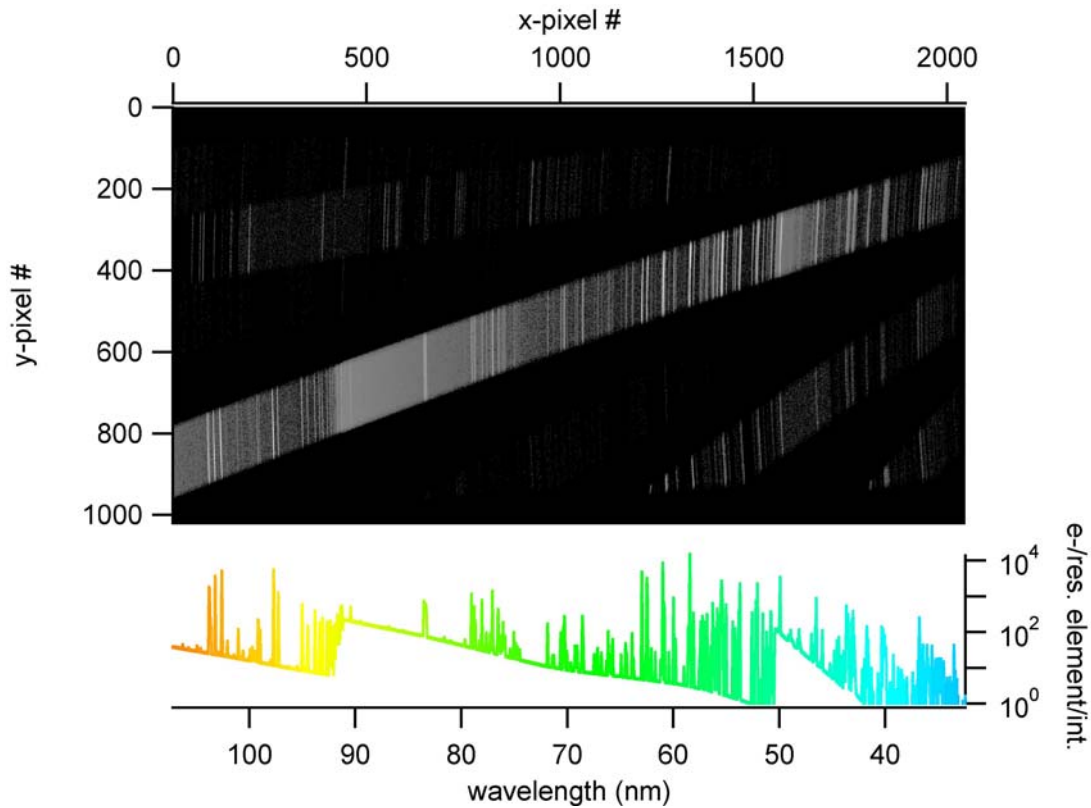


Figure 5: MEGS-B simulated detector image. The primary science (1.1) order spectrum falls diagonally across the detector from the upper right to lower left. Note that the image has been contrast-enhanced to show weaker lines. The corresponding solar signal estimate is shown below the image

A simulated CCD image of a solar spectrum taken with MEGS-B is shown in Figure 5. Again, the contrast has been enhanced to show dim lines. Wavelengths go from right to left, as indicated on below the image. The primary spectrum falls diagonally across the detector from the lower left to the upper right. Higher order spectra fall to either side of the primary spectrum. MEGS-B will be used to cover the 35 to 105 nm wavelength range.

3.2.2.1.3 MEGS Solar Aspect Monitor (MEGS-SAM) Design

The requirement for knowledge of EVE's alignments for preflight calibrations, spacecraft mounting, and solar observations is 1 arc-minute. Quadrant diodes have been used as solar aspect sensors on the TIMED SEE EGS and SORCE SOLSTICE instruments to provide pre-flight and in-flight alignment information. The Solar Aspect Monitor (SAM), although it is not a quadrant diode, serves the same purpose for MEGS. The SAM is a simple addition to the MEGS-A channel that provides alignment information for pre-flight calibration and tests and in-flight solar measurements. The optical layout of the MEGS-SAM is shown in Figure 6. SAM is a pinhole camera within the MEGS-A housing, using a separate aperture, but focusing an image of the Sun onto a portion of the MEGS-A CCD where the bandpass filter for slit 2 allows essentially no light to fall. The SAM aperture has a separate filter wheel mechanism allowing three modes. In aspect monitor mode a UV filter is in place and the resultant image of the Sun can be centroided to give pointing information for all of EVE relative to the boresights found during pre-flight calibrations to roughly 1 arcminute accuracy. In XUV photon-counting mode a Be foil filter is in place to isolate 0.1 to 5 nm. The pinhole and filter are optimized so that in this mode only single photon events occur per pixel per 10-sec CCD integration. This allows for the determination of the energy (or wavelength) of each photon event. Binning photon events from over the entire image of the Sun gives a low (~ 1 nm) spectral resolution for the SAM XUV bandpass. Summing consecutive integrations over minutes will give XUV images of the Sun. The third mode for SAM has the filter wheel in a blanked off position for dark measurements. The location and a simulated image for SAM are shown in Figure 3.

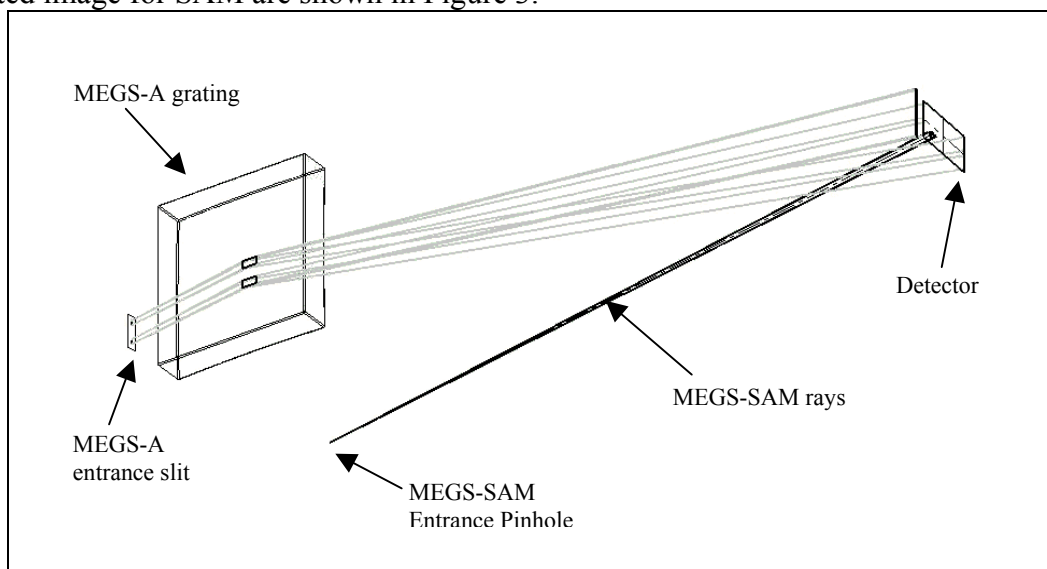


Figure 6: MEGS-SAM optical layout within the MEGS-A housing.

3.2.2.1.4 MEGS Photometer (MEGS-P) Design

The optical layout of the MEGS-P is shown in Figure 7. MEGS-P is an IRD silicon photodiode placed at the -1st order of the first MEGS-B grating. In front of the diode is an Acton interference filter to isolate the solar hydrogen Lyman- α line at 121.5 nm. The filter has a bandwidth of 10 nm, but the solar spectrum is such that greater than 99% of the signal will be due to Lyman- α . Next to the primary MEGS-P diode is an identical diode that is masked off to give simultaneous dark information that is used to correct the MEGS-P measurements for background noise induced by particle radiation.

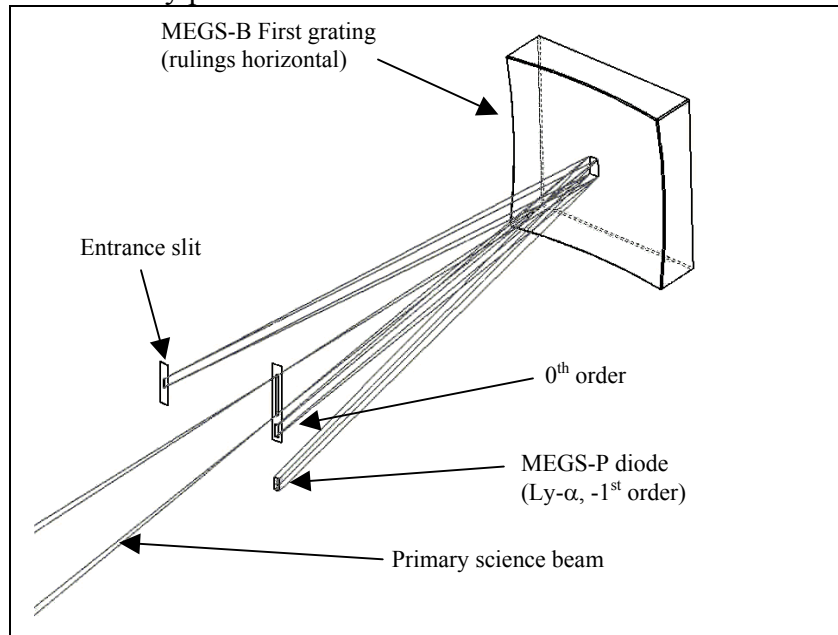


Figure 7: MEGS-P optical layout with the first chamber of MEGS-B. The photometer is placed on the opposite side of the the 0th order as the primary spectrum from the MEGS-B first grating.

3.2.2.1.5 EUV SpectroPhotometers (ESP) Design

The EUV Spectrophotometer (ESP) is a small, lightweight instrument based on the successful design of the SOHO SEM spectrometer [Judge et al., 1998]. The optical layout of the ESP is shown in Figure 8. The ESP is a non-focusing, broadband spectrograph with a transmission grating and IRD silicon photodiodes. In front of the entrance slit is an Al foil filter made by Luxel to limit the out-of-band light that gets into the instrument. The transmission grating, made by X-Opt, is essentially a set of thin wires with no substrate spaced so that there are 2500 lines/mm. Silicon photodiodes are placed at both plus and minus first orders and positioned so that the centers are at 18.2, 25.7, 30.4, and 36.6 nm. The diodes are sized to give approximately 4-nm bandpasses centered on each of these wavelengths. The central, zeroth order position has a silicon quadrant photodiode with an additional thin foil filter to isolate 0.1 to 7 nm. The sum of the quadrants gives the solar irradiance in this bandpass. Differencing the quadrants allows for determination of the pointing of the ESP. The ESP has a filter wheel mechanism with open and blanked off positions for solar and dark measurements. The ESP has the fastest measurement cadence of all of the instruments in the EVE suite at 0.25 seconds.

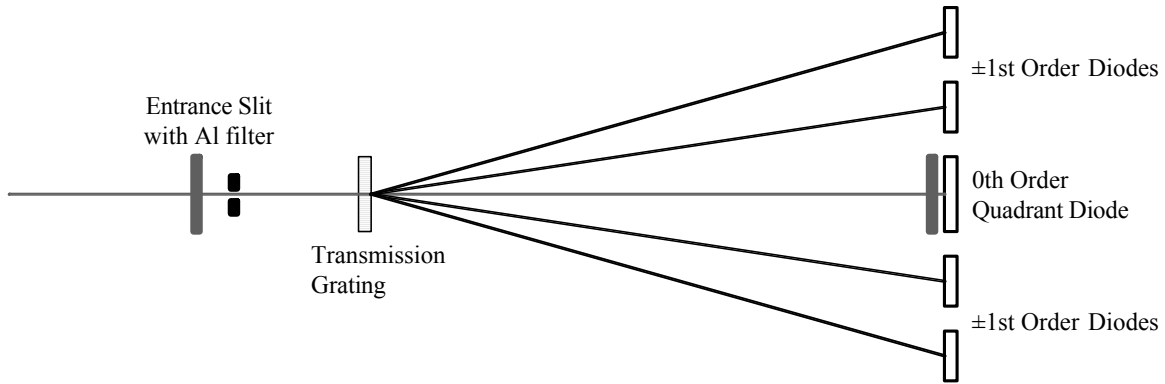


Figure 8: ESP optical layout.

3.2.3 EVE Heritage

3.2.3.1 Instrument Heritage

The MEGS Channels A and B have evolved from the successful TIMED SEE EGS instrument and from sounding rocket versions of the EGS, designed and built by LASP. The CCD cameras for MEGS consist of space-flight CCDs and associated signal processing electronics developed at the MIT Lincoln Laboratory (MIT LL). The CCD cameras have excellent heritage based upon devices flown on the Chandra ACIS instrument, Astro-D CIS instrument, and the Space Based Visible (SBV) instrument on the MSX spacecraft (DoD). Similar cameras will be flown on the HETE-II and Astro-E spacecraft. The MEGS-SAM in spectral irradiance mode utilizes a technique used for astronomical X-ray spectroscopy. The ESP is a direct descendent of the highly successful Solar EUV Monitor (SEM) built by USC and flown on the Solar Heliospheric Observatory (SOHO) and on many sounding rocket flights.

3.2.3.2 Algorithm and Calibration Heritage

The algorithms to convert spectroscopic measurements from detector signal to solar irradiances for both MEGS and ESP are essentially the same as those used in the current TIMED-SEE and SOHO-SEM data processing. LASP has extensive experience in calibrating both high resolution and broadband instruments.

4 EVE Calibration Plan

4.1 Overall Calibration Scheme

Solar EUV irradiance instruments are notoriously difficult to calibrate absolutely. Until recently there have been disagreements as large as a factor of four over the absolute irradiance at some wavelengths (particularly in the XUV). While spacecraft instruments may have good relative measurement stability (precision) that allow for comparisons between measurements made by the same instrument at different times, there has been a problem of knowing the absolute value of the irradiance being measured. The calibration philosophy for EVE has evolved from the experiences of the EVE team with measuring solar spectral irradiances from space-borne instrumentation over several decades, particularly the recent TIMED-SEE instrument.

The essentials for any absolutely calibrated spectral irradiance instrument are to 1) Calibrate pre-flight to an appropriate radiometric standard, 2) Track in-flight any changes that will affect the measurements, 3) Re-calibrate in-flight both as close as possible after launch and at regular intervals thereafter to track absolute changes, and 4) Validate with measurements made by other instrumentation and with models.

4.2 Pre-flight Calibration Plans

The EVE calibration plan includes unit level and system level calibrations. At the unit level, the individual optical elements and detectors are tested to verify they meet expectations and to select the best elements, usually based on sensitivity and uniformity. At the system level, each EVE subsystem (MEGS and ESP) is calibrated at the National Institute of Standards and Technology (NIST) Synchrotron Ultraviolet Radiation Facility (SURF) in Gaithersburg, MD as the principle pre-flight calibration. The synchrotron source provided by NIST SURF is a primary radiometric source and provides the most accurate calibration for any UV instrument. The SURF Beam Line 2 (BL-2) is dedicated for NASA instrument calibrations and includes a very large vacuum tank with a gimbal system. Furthermore, the calibration of all SDO solar UV instruments at NIST will establish a common pre-flight reference. The SURF calibrations provide sensitivities referenced to the radiometrically accurate synchrotron standard, polarization sensitivity, FOV mapping using the BL-2 gimbal table, non-linearity correction factors by adjusting the SURF beam current, and higher order corrections by using multiple SURF beam energies. By using SURF, only small calibration systems are needed elsewhere to perform unit level tests. The uncertainty of the SURF synchrotron source is less than 1%, which permits uncertainty of the instrument sensitivity of 2-7%, depending on the measurement precision and the correction factors applied in deriving the sensitivity [Eparvier et al., 2001; Woods et al., 1999].

4.2.1 MEGS Pre-flight Calibrations

At the unit level, the individual optical elements of all the MEGS channels will be characterized and verified. The slit areas will be measured with a translation microscope and with diffraction techniques. The filters will be checked for visible light leaks at LASP. The filter transmissions will be modelled by the manufacturers and verified at NIST SURF. The gratings will be characterized for reflectivity, efficiency, scattered light, and FOV variations using LASP facilities. The CCD detectors will also be characterized at LASP for flatfield response, dark noise, readout noise, integration timing, and readout timing.

At the system level, the MEGS subsystem as a whole will be exposed to XUV and EUV line sources for wavelength range verification and to the NIST-SURF beam for primary sensitivity calibration of all channels. On the SURF BL-2 vacuum and gimbal facility the MEGS channels will be individually calibrated for absolute radiometric sensitivity over their entire wavelength ranges and for FOV variability of sensitivity. Filters both internal to the MEGS-A and MEGS-B and in the beamline external to the MEGS will be used to provide information about second and third grating order contributions. In addition, multiple SURF beamline energies will also be used to determine the relative contributions to the signal from first, second, and third orders. Dark signals and detector flatfields (using internal flatfielding LEDs) will also be performed repeatedly at the system level for MEGS.

4.2.2 ESP Pre-flight Calibrations

At the unit level, the individual optical elements of the ESP will be characterized and verified. The electrometers will be tested for transfer function and linearity at USC. The filters will be checked for light leaks and the filter transmissions will be measured at NIST SURF. The grating transmissions and FOV response will also be calibrated at NIST SURF, as will the quantum yield of the ESP photodiodes.

At the system level, the ESP subsystem as a whole will be calibrated at NIST SURF for quantum throughput as a function of wavelength and FOV, similar to the MEGS subsystem.

4.3 In-flight Tracking of Short-Term Changes

During such a long mission and in the harsh environment of geosynchronous orbit, many factors can cause the response of the EVE instruments to change in-flight. These include contamination, radiation damage, exposure-related degradation, temperature effects, and so on. All EVE channels will undergo regular dark measurements. The SDO spacecraft will perform regular off-nominal pointing maneuvers to use the Sun to make maps of the EVE instrument fields of view. This will allow for corrections based on exposure “burn-in”. Both MEGS have LED lamps to perform regular flatfielding of the CCDs to track degradation of individual pixels. Two different visible wavelengths are used (separately) for flatfielding. The penetration depths of the visible wavelengths in the silicon of the CCDs are similar to those of the EUV wavelengths that MEGS is detecting.

The MEGS detectors are cooled, so can serve as traps for contaminants. The CCDs have heaters that will allow for periodic “burning off” of the detectors if necessary. Unfortunately heating can change the responsivity of the detectors; therefore, a means of tracking this sort of short term change is necessary. This is the purpose of the ESP and MEGS-P. The ESP broadband channels overlap with MEGS wavelengths and can provide a source of continuity of calibration over weeks and months. The MEGS-P at 121.5 nm does not overlap with MEGS wavelengths, but since the solar Lyman- α emission varies similarly to the hydrogen continuum (which peaks near 90 nm) and Lyman- β (at 102.6 nm), it can be used as a proxy to track changes in wavelengths that are measured by MEGS. The silicon photodiodes used in ESP and MEGS-P are considered standard radiometric detectors by NIST and so are expected to be fairly stable. In addition, overlapping wavelengths between the two slits in MEGS-A and between MEGS-A and B, and the higher order filters on MEGS also provide some level of redundancy for tracking changes.

4.4 Long-term Absolute Calibration Tracking (Re-Calibration)

Even with careful pre-flight calibration and fastidious contamination control, it is difficult to guarantee that the absolute calibration of the instrument won't change once the spacecraft has been launched and the instrument begins operations. On-board redundant or overlapping channels can only track short-term, relative changes because there is no guarantee that those channels have not undergone absolute calibration changes similar to the primary channels (such as by contamination). Some sort of periodic re-calibration to absolute standards is necessary, particularly right at the start of the mission and at regular intervals throughout. As part of the EVE project, sounding rocket versions of all the EVE channels are being built. The sounding rocket will fly soon after SDO normal operations begin and at regular intervals thereafter. The first two flights will be about 6 months apart, but later flights may have longer intervals based on

the measured changes in the spacecraft instruments. The rocket instruments will be calibrated at NIST SURF-III both before and after each rocket flight. The rocket instruments and the spacecraft instruments will make simultaneous measurements of the Sun during the rocket underflights. This allows for a transfer of absolute calibration from NIST to EVE via the rocket instruments.

4.5 Validation

The best way to validate a measurement is to make a measurement at the same time with a different instrument, preferably one that is fundamentally different in design. Unfortunately, there are not very many on-going measurements of the solar EUV. The EVE measurements will be compared to the SEE and SEM measurements, if TIMED and/or SOHO are still in operation when SDO launches. EVE will also be compared to the EUV spectrometer (EUVS) on the NOAA GOES-N satellite, if it is in operation at the time. This is a broadband instrument similar to the ESP. One can also consider the measurements of MEGS and ESP capable of validating each other, since they are fundamentally different instruments. Validation by comparisons to solar EUV models is also planned. Empirical models based on measurements from missions not necessarily overlapping with SDO can span temporal gaps, though more often comparisons between measurements and models are used to validate the model rather than the measurements.

5 EVE Measurement Algorithm Descriptions

5.1 Theoretical Basis

The purpose of the EVE instrumentation is to disperse and measure solar light. All of the EVE channels convert solar photons into electronic signals in a manner that can be quantified and calibrated. In the MEGS and ESP this conversion is accomplished by having the light fall on silicon detectors (CCDs and photodiodes). In the MEGS-A, MEGS-B, and ESP channels the solar light is limited in wavelength range by filters and dispersed spatially on the detector systems using reflection gratings (MEGS) and transmission grating (ESP). In the MEGS-P the wavelength limitation is provided by filters for the zeroth order trap photometers and by spectral dispersion from the first grating MEGS-B. In MEGS-SAM the energy (wavelength) of incident photons is determined by the method of detection itself.

To correctly determine irradiance from the measured signals sent down in EVE science telemetry, one must model the entire chain of events from incidence of solar photons on the entrance aperture of each channel all the way through to the creation of Data Numbers (DN) in the EVE electronics. Then this instrument model must be inverted to derive an algorithm which goes from signal (DN) back to irradiance in a series of steps. Each step has quantities which are known from calibration measurements or modelling, and each step has uncertainties associated with it. This section will describe the algorithms for calculating irradiance from each of the EVE channel signals.

5.2 Conversion of Instrument Signals to Irradiance Units

5.2.1 MEGS-A and MEGS-B Measurement Equations

The algorithm described in Equations 4.1 shows the derivation of solar spectral irradiance from raw signal for the MEGS-A and MEGS-B channels.

$$C_1(x,y) = \frac{S(x,y)}{\Delta t} \cdot G(T) \cdot f_{FF}(x,y,t) \cdot f_{Lin}(S) \quad (1a)$$

$$C_2(x,y) = C_1(x,y) - C_{Dark}(x,y) - C_{SL}(x,y) \quad (1b)$$

$$C_3(\lambda) = \frac{\sum_{Good(x,y)} f_{Image}(x,y) \cdot C_2(x,y)}{\sum_{Good(x,y)} f_{Image}(x,y)} \quad (1c)$$

$$E(\lambda) = \frac{C_3(\lambda)}{A \cdot \Delta \lambda \cdot R_{Center}(\lambda,t) \cdot f_{Degrad}(\lambda,t) \cdot f_{FOV}(\lambda,\theta,\phi) \cdot f_{1AU}(t)} \cdot \frac{hc}{\lambda} - E_{OS}(\lambda) \quad (1d)$$

The first step (1a) takes the raw signal, S (in DN) at a given detector location (x,y) , and converts it to the physical units of electrons (e-) with the gain factor, G (in e-/DN) which is a function of the temperature, T . This is then divided by the integration time to give e-/sec. Then a correction factor, f_{FF} , for flat-field effects is applied, as is a linearity correction, f_{Lin} . The second step (1b) is to apply subtractive corrections for dark count rate, C_{Dark} , and scattered light, C_{SL} .

Next (1c), since the slit image on the detector falls on hundreds of pixels, a weighted average is taken over all the pixels in the non-dispersive direction which have the same wavelength incident. At this time any pixels that are deemed to be bad by reason of damage or spurious signal due to high-energy particles are excluded from the average (hence the “ $Good(x,y)$ ” for the range of the summations). The weighting, f_{Image} , is based on the relative contribution of each pixel to the slit image on the detector.

Finally (1d), this corrected count rate for wavelength λ is converted to irradiance ($W m^{-2} nm^{-1}$) by dividing by the area of the slit, A (in m^2), the dispersion, $\Delta \lambda$ (in nm), the detector responsivity at the center of the field of view, R_{Center} , a degradation factor, f_{Degrad} , and a field-of-view correction factor, f_{FOV} , a normalization factor to 1 AU, f_{1AU} , and then multiplied by a factor of hc/λ to convert from photon units to energy units. At this point an order-sorting correction, E_{OS} , is applied to remove second and higher order contributions from the spectrum.

The degradation of the MEGS is actually tracked through three functions: daily flatfield images (f_{FF}), weekly degradation (f_{Degrad}) from comparisons to redundant channel measurements (ESP and MEGS-P), and regular sounding rocket calibrations (adjusted R_{Center}). The flat-field correction is derived from the flat-field images taken most recently in flight that are normalized using the pre-flight flat-field image. The flat-field function, therefore, includes the local degradation on the CCD that should primarily occur at the brighter emissions. The weekly degradation function is derived using trends in the ratios of the MEGS irradiances to the ESP and MEGS-P irradiances. For transfer of the rocket results to MEGS, the responsivity is adjusted for the MEGS so that its irradiances on the rocket flight dates match the rocket irradiances. A model based on multiple rocket comparisons (when they become available) is used to interpolate between rocket dates.

5.2.2 MEGS-SAM Measurement Equation

Equation 2 describes the derivation of the solar irradiance for the MEGS-SAM in spectral mode. Similar to the final step of the MEGS algorithm, the SAM algorithm is a straightforward calculation converting detector signal to irradiance, but with fewer correction factors because of its simpler optical design and because the detector registers each photon event individually. The wavelength, λ , is determined from the number of electrons of each photon event.

$$E(\lambda) = \frac{S(\lambda) \cdot G \cdot f_{FF}(x, y, t) \cdot f_{Lin}(S)}{\Delta t \cdot A \cdot \Delta \lambda \cdot R(\lambda) \cdot f_{Degrad}(\lambda, t) \cdot f_{IAU}(t)} \cdot \frac{hc}{\lambda} \quad (2)$$

Here S is the sum of all the signals from all the pixels in the SAM region of the detector which are associated with a bandpass of $\lambda - \Delta\lambda/2$ to $\lambda + \Delta\lambda/2$, G is the gain, f_{FF} is the flatfield correction, f_{Lin} is the linearity correction, Δt is the integration time, A is the pinhole area, R is the responsivity, f_{Degrad} is a degradation function, and f_{IAU} is a scaling to a constant distance from the Sun. The responsivity includes the quantum efficiency of the CCD and the transmission of the X-ray filter. A SAM irradiance spectrum is essentially built up as a histogram of photon events with the same energies (wavelengths).

5.2.3 ESP and MEGS-P Measurement Equation

The irradiance algorithm is essentially the same for both the ESP and the MEGS-P and is given by Equation 3.

$$E(\lambda) = \frac{S(t) - S_{Dark}}{A \cdot \sum [R(\lambda) \cdot f_{Weight}(\lambda) \cdot f_{Degrad}(\lambda, t) \cdot \Delta\lambda]} \cdot \frac{hc}{\lambda} \quad (3)$$

Here S is the count rate from the diodes, S_{Dark} is the dark count rate, A is the aperture area, R is the responsivity of the diode, f_{Weight} is the weighting of the spectral flux within the bandpass ($\Delta\lambda$) of the diode, f_{Degrad} is a correction for degradation, and f_{IAU} is the normalization to 1 AU distance. The summation is over the bandpass of the diode. The weighting functions are determined with Equation 4.

$$f_{Weight}(\lambda) = \frac{F(\lambda)}{\int_{\Delta\lambda} F(\lambda) \cdot d\lambda}, \quad (4)$$

where $F(\lambda)$ is either an assumed spectral distribution or one measured by MEGS-A or B over the bandpass of the ESP or MEGS-P photometer. In the cases where a filter is in front of the diode, the spectral distribution, $F(\lambda)$, is multiplied by the transmission function, $\tau(\lambda)$, of the filter.

5.3 Signal Estimates and Error Analyses for Subsystems

5.3.1 MEGS Signal Estimates and Error Analysis

Computer models of the anticipated response to solar incident light for each of the MEGS spectral channels have been made. These models include slit functions, filter transmissions, grating reflectivities, grating efficiencies, grating dispersion properties, optical imaging properties, and detector sensitivities as they were known in the design phase of the project. The models were given representative solar incident spectra for solar minimum, solar maximum, and

solar flare conditions, as provided by the NRLEUV solar spectral model. In addition, noise estimates were made for each of the MEGS channels including anticipated CCD read-out noise, dark current, fano noise (important for the shorter wavelengths), analog-to-digital conversions, and counting statistical noise. Figures 9, 10, and 11 show the estimated signals in each of the MEGS spectral channels for solar minimum, solar maximum, and solar flare conditions. The signals shown are in electrons per 10-sec integration in a single pixel. The End of Life signal requirement is at around 20 and is the estimated minimum brightness needed for one of the required 18 lines to meet the 25% uncertainty requirement by the end of the mission, given estimated degradation. There are many more than 18 lines which meet this requirement.

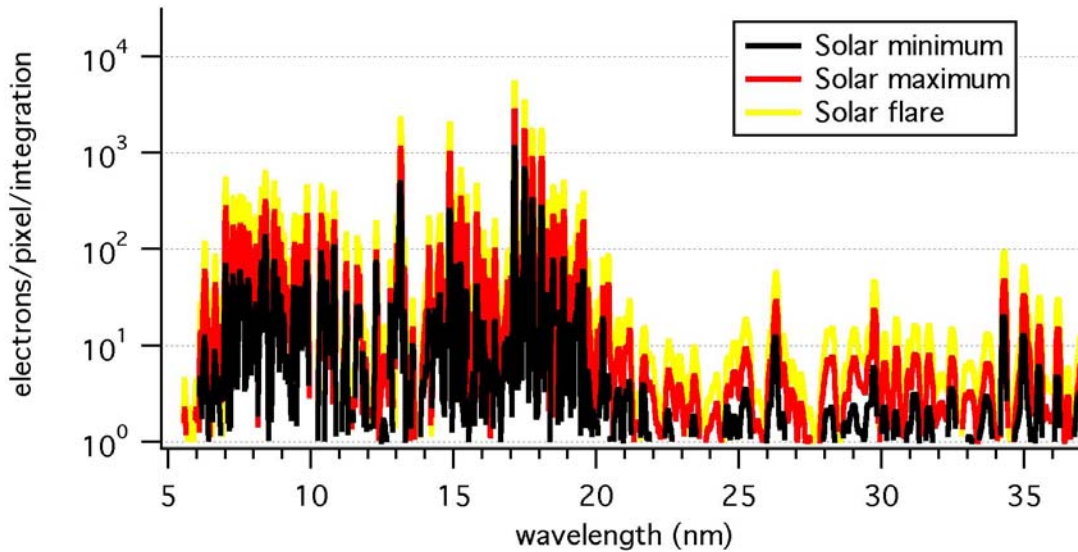


Figure 9: MEGS-A Slit 1 signal estimates for solar minimum, maximum, and flare conditions.

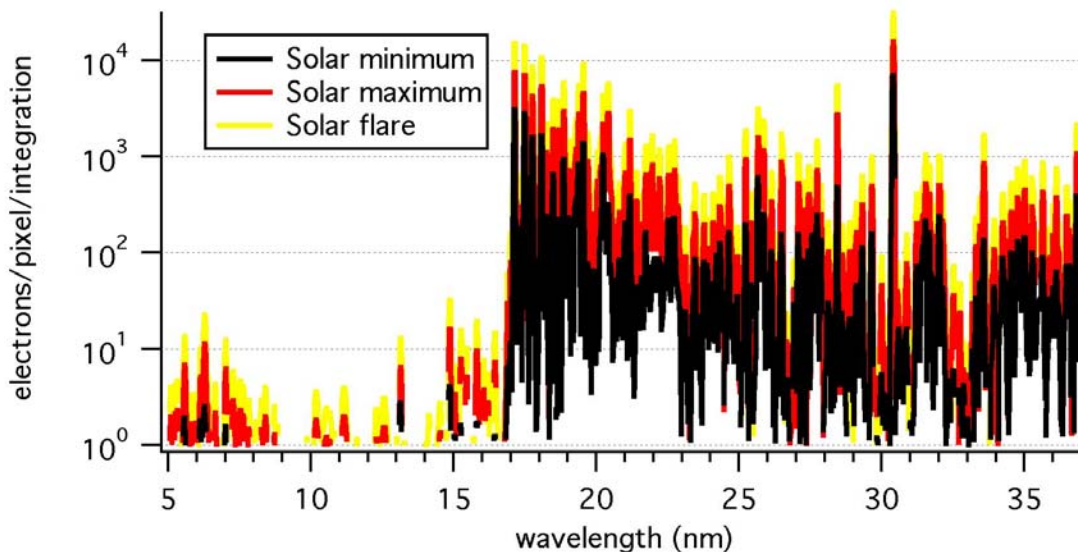


Figure 10: MEGS-A Slit 2 signal estimates for solar minimum, maximum, and flare conditions.

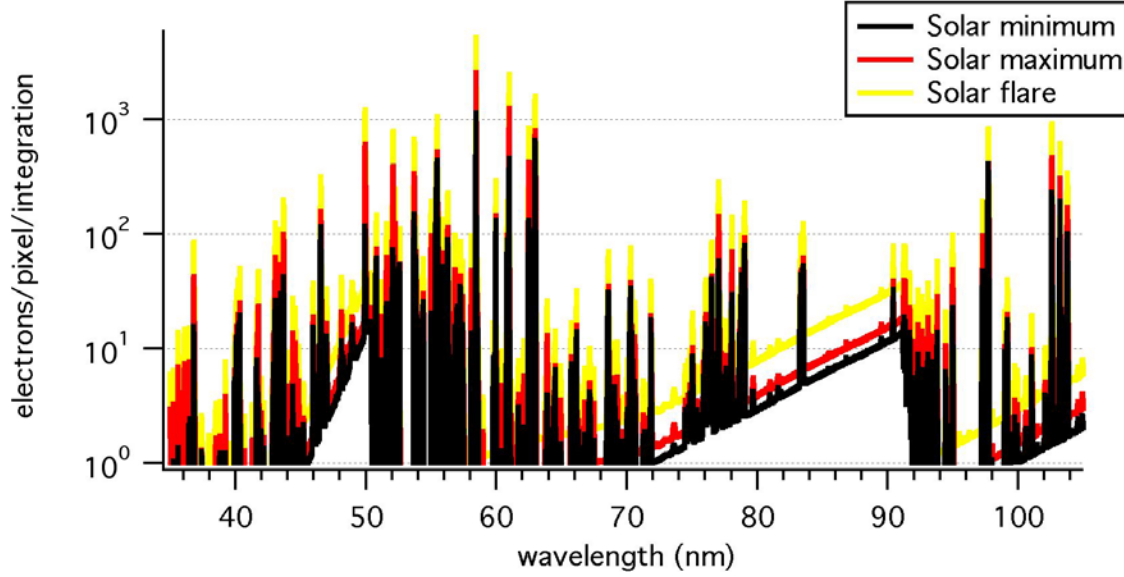


Figure 11: MEGS-B signal estimates for solar minimum, maximum, and flare conditions.

The propagation of uncertainties through the irradiance algorithms (Equations 4.1) for MEGS-A and MEGS-B is given in Equations 5, where σ_{var} represents the uncertainty of a variable var , in the units of var .

$$\sigma_{C_1}^2 = C_1^2 \cdot \left[\frac{\sigma_S^2}{S^2} + \frac{\sigma_{\Delta t}^2}{\Delta t^2} + \frac{\sigma_G^2}{G^2} + \frac{\sigma_{f_{FF}}^2}{f_{FF}^2} + \frac{\sigma_{f_{Lin}}^2}{f_{Lin}^2} \right] \quad (5a)$$

$$\sigma_{C_2}^2 = \sigma_{C_1}^2 + \sigma_{C_{Dark}}^2 + \sigma_{C_{SL}}^2 \quad (5b)$$

$$\sigma_{C_3}^2 = \sum_{\text{Good}(x,y)} \left\{ \left[\frac{f_{Image}(x,y) \cdot C_3}{\sum_{\text{Good}(x,y)} f_{Image}(x,y)} \right]^2 \cdot \left[\frac{\sigma_{f_{Image}(x,y)}^2}{(f_{Image}(x,y))^2} \cdot \left(1 - \frac{f_{Image}(x,y)}{\sum_{\text{Good}(x,y)} f_{Image}(x,y)} \right) + \frac{\sigma_{C_2(x,y)}^2}{(C_2(x,y))^2} \right] \right\} \quad (5c)$$

$$\sigma_E^2 = E^2 \cdot \left[\frac{\sigma_{C_3}^2}{C_3^2} + \frac{\sigma_A^2}{A^2} + \frac{\sigma_{\Delta\lambda}^2}{\Delta\lambda^2} + \frac{\sigma_{R_{Center}}^2}{R_{Center}^2} + \frac{\sigma_{f_{Degrad}}^2}{f_{Degrad}^2} + \frac{\sigma_{f_{FOV}}^2}{f_{FOV}^2} + \frac{\sigma_{f_{IAU}}^2}{f_{IAU}^2} + \frac{\sigma_{\lambda}^2}{\lambda^2} \right] + \sigma_{E_{os}}^2 \quad (5d)$$

The measurement precision, being the uncertainty for a single measurement, is represented by equation 5c. The absolute accuracy, being the uncertainty for the absolute value of the irradiance from a single measurement, is given by equation 5d.

Table 3s shows an error propagation for an “acceptable” spectral line, which is defined as the dimmest spectral line (with a margin of a factor of two) that we deem to be still usable to meet our science objectives as one of the 18 solar lines to measure through the life of the mission. The estimated uncertainty for such a line is about 13%. The final column of the table is an estimated breakdown of the error budget allowable for each parameter in the measurement equation to meet the 25% requirement for the mission.

Table 3: MEGS-A and MEGS-B Uncertainty Estimate and Error Budget

Parameter	Value for “Acceptable” spectral line	Uncertainty Estimate (“Acceptable” spectral line)	Error Budget (allowable error)
$S(x,y)$	12 DN/pix	2 DN/pix (17%)	34%
Δt	10 s	0.001 s (0.01%)	0.02%
$G(T)$	2.0 e-/DN	0.5%	1%
$f_{FF}(x,y,t)$	1.0	1%	2%
$f_{Lin}(S)$	1.0	0.1%	0.2%
$C_I(x,y)$	2.4 e-/s/pix	0.4 e-/s/pix (17%)	34%
$C_{Dark}(x,y)$	0.2 e-/s/pix	0.02 e-/s/pix (10%)	20%
$C_{SL}(x,y)$	0.2 e-/s/pix	0.02 e-/s/pix (10%)	20%
$C_2(x,y)$	2.0 e-/s/pix	0.16 e-/sec/pix (8%)	16%
$f_{Image}(x,y)$	1	1%	2%
$Good(x,y)$	100 pix	-	-
$C_3(\lambda)$	200 e-/s	1.6 e-/s (0.8%)	1.6%
A	$4 \times 10^{-8} \text{ m}^2$	$1.6 \times 10^{-9} \text{ m}^2$ (4%)	8%
$\Delta \lambda$	0.1 nm	0.003 nm (3%)	6%
$R_{Center}(\lambda,t)$	1 e-/ph	0.06 e-/ph (6%)	12%
$f_{FOV}(\lambda, \theta, \phi)$	1.0	5%	10%
$f_{Degrad}(\lambda,t)$	0.95	9%	18%
$f_{IAU}(t)$	1	0.01%	0.02%
λ	20 nm	0.02 nm (0.1%)	0.2%
$E_{OS}(\lambda)$	$10^{-4} \text{ W/ m}^2/\text{nm}$	1%	2%
$E(\lambda)$	$5 \times 10^{-8} \text{ W/ m}^2/\text{nm}$	$0.65 \times 10^{-8} \text{ W/ m}^2/\text{nm}$ (13%)	25%

5.3.2 MEGS-SAM Signal Estimates and Error Analysis

Figure 12 shows the estimated signal for the MEGS-SAM in irradiance mode, using a solar spectral input for solar minimum conditions, and binning the signal into 1 nm intervals.

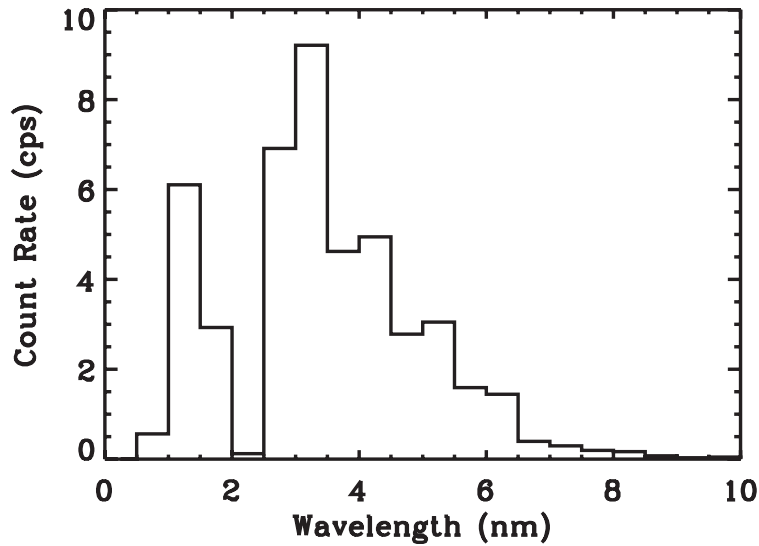


Figure 12: MEGS-SAM irradiance signal estimates for solar minimum conditions.

The spectral resolution of the SAM X-ray spectrum is limited by the CCD pixel noise and Fano noise (deviation from the nominal electron per 3.65 eV of photon energy). The energy (spectral) resolution, Δe in eV, is given by:

$$\Delta e = (2.355) \cdot \sqrt{\left(3.65 \frac{eV}{e^-} \cdot G \cdot \sqrt{S_{Dark}}\right)^2 + \frac{hc}{\lambda} \cdot F_a} \quad (6)$$

where the first term under the square root is the dark noise (about $2 e^-$), and the second term is the Fano noise, with F_a as the Fano factor of about 0.1 for silicon [Janesick, 2001]. For the SAM the ideal energy resolution varies from 41 eV (0.008 nm) at 0.5 nm and 20 eV (0.7 nm) at 6.5 nm. Because individual photon events are recorded in the CCD image, the binning of the X-ray spectrum is done in the data processing on the ground and thus is not on any specific wavelength grid. It is currently planned to bin the SAM X-ray spectrum into 1 nm intervals (0-7 nm) in order to achieve < 10% measurement precision within each 10-sec integration period of the MEGS-A CCD. The estimated SAM count rate in these 1-nm intervals is shown in Figure 12. The size of the pinhole diameter is determined from the requirement to keep the probability of two photon events in a single CCD pixel below 10% per CCD image. The resulting pinhole diameter is 25 μm , and the SAM count rate is expected to vary between 100 and 300 counts per second (cps) for solar minimum and maximum conditions, respectively.

The measurement precision, being the uncertainty for a single measurement, is the standard photon counting uncertainty of \sqrt{S} . The typical measurement precision is expected to be less than 10% for a single 10-sec integration but can be improved by merging counts from additional integration periods.

The absolute accuracy, being the uncertainty for the absolute value of the irradiance from a single measurement, is given by equation 7. The largest source of uncertainty for the MEGS irradiance accuracy is the uncertainty of the pre-flight sensitivity, which should be less than 15%. The error budget (uncertainty) for each parameter is listed in Table 4.

$$\sigma_E^2 = E^2 \cdot \left[\frac{\sigma_S^2}{S^2} + \frac{\sigma_G^2}{G^2} + \frac{\sigma_{\Delta t}^2}{\Delta t^2} + \frac{\sigma_A^2}{A^2} + \frac{\sigma_{\Delta \lambda}^2}{\Delta \lambda^2} + \frac{\sigma_R^2}{R^2} + \frac{\sigma_{f_{Degrad}}^2}{f_{Degrad}^2} + \frac{\sigma_{\lambda}^2}{\lambda^2} \right] \quad (7)$$

The degradation of SAM is primarily tracked through ESP 0.1-7 nm irradiance measurements, as well as, longer-term degradation is tracked using the bi-annual rocket calibrations (adjusted R).

Table 4: MEGS-SAM Uncertainty Estimate and Error Budget

Parameter	Range	Uncertainty
S	30-300 DN	5-17 DN
G	1.95-2.05 e-/DN	0.1%
Δt	10 sec	0.001 sec
A	0.002 mm ²	0.0001 mm ²
$\Delta \lambda$	1 nm	0.01 nm
R	0.005-0.05	15-20%
f_{Degrad}	0.5-1.0	5%
λ	0-7 nm	0.01-0.7 nm
E	2-36 $\mu\text{W}/\text{m}^2/\text{nm}$	17-30%

5.3.3 ESP Signal Estimates and Error Analysis

The estimated uncertainties and their sources for ESP measurements are given in Table 5. For moderate solar activity the zero order detector will register ~ 180 pA, and the signal for each 1st order detectors is ~ 15 pA, based on SOHO experience. The Si photodiodes are unbiased; therefore, only Johnson noise is expected. At a temperature of 20° C and with a shunt resistance of 100 M Ω , the thermal noise will only amount to 13 f A/Hz^{1/2}. The noise in an ESP-like instrument due to ambient particles has been analyzed by Ogawa and Judge [1995a and 1995b] for the GOES missions. This study has been updated to encompass the ESP, and is included with this CSR. The study considered silver, as an example, and trade studies on the optimum shielding strategy are underway. The results of these studies have been adapted to the ESP. Local detector shielding, and spot shielding with Al/Ta/Al on the case and internal baffles will reduce the radiation induced signal to less than 0.5pA giving a SNR of about 30 for all the wavelength bands of interest.

Table 5: ESP Uncertainty Estimate and Error Budget

Source		Notes
Calibration	5%	NIST
Spectral Distribution	5%	MEGS
Aperture Area	0.05%	JPL
Weak Line Statistics	15%	
Strong Line Statistics	1%	
Irradiance Uncertainty (Weak Line)	16.6%	
Irradiance Uncertainty (Strong Line)	7.1%	

5.4 Preflight Calibration Algorithms

Calibrating an instrument at NIST-SURF is fairly straightforward. The EVE subsystems are placed in the beamline 2 and aligned to be centered in horizontal, vertical, and FOV angles. The measurement equations for each of the EVE subsystems (Equations 1, 2, and 3) are solved for the responsivity at the center, R_C , and knowing the irradiance, E , of the beamline incident on the instrument aperture, which is provided by NIST-SURF staff. Using a gimbal, the FOV can be mapped out and the f_{FOV} can be obtained by ratioing with the responsivity at the center of the FOV. Note that since the same slits are used during calibration and in flight, the area of the slits, A , actually is not relevant to the calibration or measurement except that it be large enough to give good signals and of the appropriate width for the resolution of the instrument.

APPENDIX A: List of EVE Variable Definitions

General Rules: Indicate dependence of one variable on another by parentheses (eg. $R(x)$ means that R depends on x). Use subscripts to further clarify or identify a variable (eg. R may be a responsivity, but R_{Center} is the responsivity at the center of the FOV).

A = area of aperture (slit, pinhole, ...) (m^2)

C_{Name} = quantities with dimensions of count rate (counts/sec = cps = e-/sec)

$C_{Analyzer}$ = analyzer count rate (cps)

C_{Corr} = corrected count rate (cps)

C_{Dark} = dark signal correction (cps)

C_{Part} = particle noise correction (cps)

C_{SL} = scattered light correction (cps)

C_{OS} = higher grating order correction (cps) (unless done at irradiance level)

χ = cross section (m^2)

e = energy (eV or Joules)

e_I = ionization energy

e_{KE} = kinetic energy

e_p = photon energy ($= hc/\lambda$)

E = spectral irradiance in energy units (W/m^2 or $W/m^2/nm$)

F = spectral irradiance in photon units (flux) ($photons/m^2/sec$ or $photons/m^2/sec/nm$)

f_{Name} = dimensionless correction factors

f_{IAU} = 1 AU correction

f_{Degrad} = degradation correction

f_{Weight} = flux-weighted contribution function of wavelength to bandpass (was β)

f_{Image} = weighted contribution function of pixel to slit image for MEGS

f_{FF} = flatfield correction

f_{FOV} = Responsivity variation over FOV

f_{Lin} = linearity correction (function of signal)

G = gain (function of temperature, T) in e-/DN

hc/λ = conversion from photon to energy units

I = current (amperes)

λ = wavelength (nm)

$\Delta\lambda$ = bandpass or wavelength interval or dispersion (nm)

n = number density of a gas (m^{-3})

R = Responsivity, sensitivity, or quantum yield (cnt/ph or DN/ph or e-/ph)

S = raw signal (DN)

σ_{var} = error or uncertainty of var in the units of var

Ψ_{var} = error or uncertainty of var as a fraction of 1 ($\Psi_{var} = \sigma_{var}/var$)

t = time (sec)

Δt = integration time (sec)

τ = transmission (dimensionless)

T = temperature ($^{\circ}\text{C}$ or Kelvin)

θ, ϕ = angular pointing within FOV (degrees)

x, y = pixel location on a 2-D detector with x in dispersion direction